Classification
*Physics Abstracts*
76.60 — 71.45G — 71.15N

# Electron-proton couplings and local susceptibilities in TTF and TCNQ salts

F. Devreux (*), Cl. Jeandey (*), M. Nechtschein (*)

Section de Résonance Magnétique, Département de Recherche Fondamentale, Centre d'Etudes Nucléaires de Grenoble, 85 X, 38041 Grenoble Cedex, France

J. M. Fabre and L. Giral

Laboratoire de Chimie Organique Structurale, USTL, 34060 Montpellier, France

(*Reçu le 13 décembre 1978, accepté le 13 mars 1979*)

**Résumé.** — Les raies de RMN des protons de différents composés de TTF et de TCNQ sélectivement deutériés ont été enregistrées à 250 MHz. Une évaluation du couplage hyperfin isotrope ($a$) est obtenue à partir du déplacement paramagnétique de la raie, tandis que le second moment conduit à une détermination expérimentale du couplage dipolaire ($d$). On montre que le couplage dipolaire n'est pas négligeable, aussi bien pour TTF que pour TCNQ. Pour ces deux molécules on arrive à $d \simeq \frac{1}{2} a = 0{,}6$ gauss. Par ailleurs, on donne des déterminations des susceptibilités locales dans TTF TCNQ et NMP TCNQ.

**Abstract.** — Proton NMR lines have been recorded at 250 MHz in different selectively deuterated TTF and TCNQ compounds. An evaluation of the isotropic hyperfine coupling ($a$) is obtained from the paramagnetic shift of the line, while the second moment leads to an experimental determination of the dipolar coupling ($d$). It is established that the dipolar coupling for TTF and TCNQ protons is not at all negligible. For both molecules one has $d \simeq \frac{1}{2} a = 0.6$ gauss. Further, estimates of the local susceptibilities in TTF TCNQ and NMP TCNQ are given.

1. **Introduction.** — In recent years, valuable information about the electronic properties of one-dimensional (1-D) conductors has been obtained from NMR experiments. Static (CW) measurements provide information on the local static susceptibility [1, 2], while dynamic measurements (nuclear relaxation) allow one to study the spin dynamics, which display singular features in 1-D systems [3, 4, 5]. However, difficulties arise for performing quantitative studies because the electron-proton couplings which are involved in the expression of the nuclear relaxation time ($T_1$) are not well known for tetracyanoquinodimethane (TCNQ) and tetrathiofulvalène (TTF), two basic molecules for 1-D conducting compounds. An attempt has been performed to calculate the electron-proton couplings in a TCNQ salt [6]. In the present work we present an experimental determination of the electron-proton couplings in $TCNQ^-$ and $TTF^+$ in the solid state. The values have been extracted from the proton NMR lines of powdered samples. The scalar and the dipolar couplings have been determined from the first and the second moment of the lines, respectively. Further, our experiments allow us to estimate the local susceptibility in TTF and TCNQ chains in compounds where it is unknown (e.g. compounds with two different magnetic chains).

2. **Experimental.** — The compounds studied are listed in table I, where the stars denote deuterated molecules. The selective deuteration enables us to

Table I. — Cu BDT = $CuS_4C_4(CF_3)_4$ ; $\varphi = C_6H_5$ ; Qn = *Quinolinium* ; NMP = N *méthyl-phenazinium* ; TMA = *Tetra methyl-ammonium*.

| TTF protons | TCNQ protons |
|---|---|
| TTF Cu BDT | $\varphi^*$ $CD_3As$ $TCNQ_2$ |
| TTF TCNQ* | Qn* $TCNQ_2$ |
| | TTF* TCNQ |
| | (NMP)* TCNQ |
| | $Cs_2$ $TCNQ_3$ |
| | $(TMA)^*_2$ $TCNQ_3$ |

(*) C.N.R.S., E.R., n° 216.

Article published online by EDP Sciences and available at http://dx.doi.org/10.1051/jphys:01979004007067100

observe only the protons of TTF (left hand side), or only the TCNQ protons (right hand side). The measurements were performed with a 250 MHz high resolution NMR spectrometer (Cameca 250). The derivative of the NMR line was recorded after lock-in detection, and directly digitised and integrated using an HP 9825 computer. Great attention was given to the adjustment of the RF phase in order to avoid distortion of the line. Recorded lines and absorption curves for Cu BDT TTF, $\varphi^{*}_{3}$ $CD_3As$ $TCNQ_2$ and $Cs_2$ $TCNQ_3$ at room temperature are shown in figure 1. In each case, the lineshape is highly non-Gaussian and displays significant features. For Cu BDT TTF, where the susceptibility is large ($\sim 10^{-3}$ emu/mole), the linewidth mainly arises from the anisotropic part of the hyperfine coupling. The lineshape (Fig. 1*a*) is indeed typical of an almost axially symmetric hyperfine interaction [7]. On the other hand, the susceptibility is quite negligible in $Cs_2$ $TCNQ_3$ ($\sim 10^{-5}$ emu/mole) where the main contribution to the linewidth comes from the nucleus-nucleus dipolar interaction. Actually a Pake doublet is clearly visible in figure 1*c*.

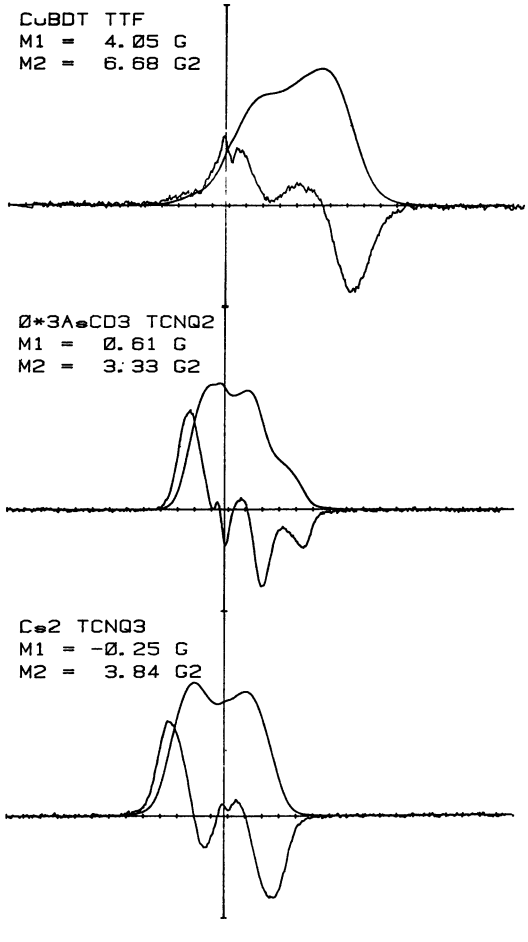


Fig. 1. — NMR spectra and absorption curves for *a*) Cu BDT TTF ; *b*) $\varphi^{*}_{3}$ $CD_3As$ $TCNQ_2$, and *c*) $Cs_2$ $TCNQ_3$. The spectra have been recorded on powdered samples at 250 MHz with a CAMECA 250 spectrometer.

The distance between the two peaks ($\sim$ 3.5 G) is exactly that which is expected for protons separated by 2.3 Å [8]. For the other compounds, whose susceptibility at room temperature is intermediate ($\sim 2 \times 10^{-4}$ emu/mole), the lineshape arises from a mixing of the proton-proton coupling and the anisotropic hyperfine coupling. This is seen in figure 1*b* for $\varphi^{*}_{3}$ $AsCD_3$ $TCNQ_2$. There is also in almost all spectra a weak, sharp line, partially saturated, which is believed to arise from solvent inclusion in the compound.

The first moments of the lines have been calculated with respect to a common reference (the proton NMR line of a rubber sample). As we shall see lateron, it should be noticed that the absolute position of the reference line does not matter for the present studies.

The second moment $M_2$ has been also calculated. It is difficult to obtain an absolute determination of $M_2$, because the calculated value depends on the integration range, due to the noise in the wings of the line. We have chosen the integration range to be symmetric with respect to the centre of the line and proportional to $M_2^{1/2}$. The proportionality constant was the same for all the spectrum and was chosen to give the best result for the second moment of a simulated randomized curve, having the same level of noise as the experimental ones. In this way we think that we have obtained a reasonable estimate of the absolute value of $M_2$. Above all, we expect that the relative values of $M_2$ for different spectra having the same shape are quite significant.

3. **Isotropic paramagnetic shift.** — The isotropic shift of the NMR line $\Delta H$ for a powdered sample in a static field $H$ is expressed as

$$\frac{\Delta H}{H} = \frac{\gamma_e}{\gamma_N} a\chi \qquad (1)$$

where $\gamma_e/\gamma_N$ is the ratio of the electronic and nuclear gyromagnetic factors ($\gamma_e/\gamma_N = -658$ for protons), $a$ is the isotropic hyperfine coupling and $\chi$ is the reduced susceptibility expressed in reciprocal energy units. It is related to the usual molar susceptibility $\chi_M$ by the expression : $\chi_M = \mathcal{N}(g\mu_B)^2 \chi$, with conventional notations.

The principle of our measurements follows from eq. (1) :

i) If the susceptibility is known from other methods, one obtains an evaluation of the coupling $a$ in the solid state.

ii) Assuming that $a$ has the same value for a given molecule in different solid state structures one can determine the local susceptibility on this given molecule.

It should be noticed that assumption ii) cannot be strictly valid ; for one thing the spin density distribution depends on the geometry of the molecule as shown by MO calculations for TCNQ [7] and the

geometry of molecules (TTF ou TCNQ) varies in the solid state from one compound to another. However, assumption ii) is taken for simplicity and it is reasonably thought to be a better approximation than the one previously used according to which $a$ had the same value in the solid state as in solution.

3.1 SCALAR COUPLING DETERMINATION. — The first moment has been determined for Cu BDT TTF and $\varphi_3^*$ $CD_3As$ $TCNQ_2$ as a function of the temperature in the range 150-350 K. These two compounds have been selected for the following reasons : i) it is quite sure that the whole susceptibility is located on the TTF and TCNQ chains, respectively ii) the susceptibility displays a significant variation with the temperature.

Thus, the paramagnetic shift $\Delta H$ can be scaled *versus* the susceptibility, using the temperature as an implicit parameter. The scalar coupling $a$ is given by the slope of the resulting straight line, using eq. (1). This is shown in figures 2*a* and *b* for $\varphi_3^*$ $CD_3As$ $TCNQ_2$ and Cu BDT TTF, respectively. Actually, when the temperature decreases, the susceptibility (and the shift) increases in Cu BDT TTF, while it decreases in $\varphi_3^*$ $CD_3As$ $TCNQ_2$. The values of the spin susceptibility as a function of the temperature have been taken from Jacobs *et al.* [10] and from Kepler [11] for the TTF compound and for the TCNQ compound, respectively. Error bars in the figures are evaluated from r.m.s. deviation of several (3 to 6) measurements. Since only the slope of the variation $\Delta H$ *versus* $\chi$ plays a role in our determination, one does not have to consider its absolute value.

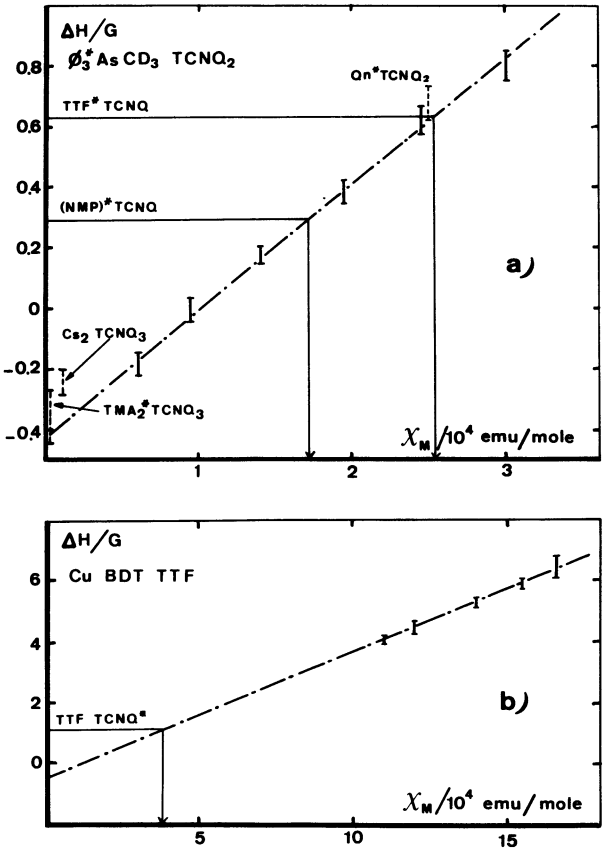


Fig. 2. — Shifts of the NMR line of (*a*) the TCNQ protons in different TCNQ compounds and (*b*) the TTF protons in different TTF compounds. The shifts have been measured with respect to a common reference : the NMR line of a rubber sample.

However, it should be noticed that the chemical (diamagnetic) shift of the rubber and of TCNQ or TTF cannot be considered to be the same. The obtained scalar couplings are :

$$a_F/\hbar \,|\, \gamma_e \,| = -1.2 \text{ G}$$

$$a_Q/\hbar \,|\, \gamma_e \,| = -1.2 \text{ G}$$

for TTF and TCNQ respectively. These values have to be compared to the values measured by EPR in solution : 1.26 [12] and 1.4 [13] G for TTF and TCNQ respectively. Our evaluation for $a_Q$ is in relative agreement with the value obtained by Kuindersma [14] in MEM $TCNQ_2$ (MEM = méthyl-ethyl-morpholinium), but it disagrees with that obtained by Schegolev *et al.* [15] at low temperature in Qn $TCNQ_2$. However, it seems that in that case inhomogeneous effects play an important role and should modify the interpretation of the results [16]. For the other compounds listed in table I, the room temperature paramagnetic shifts have also been plotted in figure 2. For the compounds whose susceptibility is known to be located only on the TCNQ stacks ($Cs_2$ $TCNQ_3$, Qn* $TCNQ_2$, $TMA_2^*$ $TCNQ_3$) the results are consistent with the value of $a_Q$ obtained in $\varphi_3^*$ $CD_3As$ $TCNQ_2$, within the experimental accuracy. This shows that the isotropic hyperfine coupling is fairly closely the same among different solid state structures and different degrees of charge per site.

3.2 LOCAL SUSCEPTIBILITY DETERMINATION. — Let us turn now to the second utilization of the paramagnetic shift measurements. Assuming the values for $a_Q$ and $a_F$ previously determined from the paramagnetic shift, one may deduce the local susceptibility. First, one may note that the plot of Qn* $TCNQ_2$ in figure 2*a* is consistent with complete charge transfer for this compound as previously shown [17, 18, 19]. More interesting are the results in compounds whose total susceptibility arises from two contributions, involving incomplete charge transfers : TTF TCNQ and NMP TCNQ. Taking for $a_Q$ and $a_F$ the values previously determined, the paramagnetic shift measurements in (NMP)* TCNQ, TTF* TCNQ and TTF TCNQ* give the following results for the room temperature local susceptibilities :

$$\text{NMP TCNQ} : \chi_Q = (1.7 \pm 0.15).10^{-4} \text{ emu/mole}$$

$$\text{TTF TCNQ} : \chi_Q = (2.5 \pm 0.15).10^{-4} \text{ emu/mole}$$

$$\text{TTF TCNQ} : \chi_F = (3.8 \pm 0.20).10^{-4} \text{ emu/mole}$$

In TTF TCNQ, evaluations of the local susceptibility have been performed already from the angular and temperature dependence of the $g$ factor [20] and from the $^{13}C$ paramagnetic shift in selectively enriched compounds [21]. Our results are in better agreement with those obtained from EPR. In the case of NMP TCNQ our data provide the first evaluation of the local susceptibility. The TCNQ susceptibility in NMP TCNQ appears relatively small as compared to the other conducting TCNQ chains (see Fig. 2). This may be partially caused by the different band filling, an estimate of which can be obtained as follows. From the value of the total susceptibility $(4.9 \pm 0.7).10^{-4}$ emu/mole (measured on the same sample using a conventional vibrating sample magnetometer), the NMP stack susceptibility is deduced as : $(3.2 \pm 0.85).10^{-4}$ emu/mole. Assuming a Curie susceptibility in the NMP stacks at room temperature, as consistent with the narrowness of the spin fluctuation spectrum (< 10 K) [22], one obtains the concentration of spin 1/2 paramagnetic centres on the NMP stacks : $C \simeq 0.25 \pm 0.06$. This result is in qualitative agreement with our previous estimate based upon the analysis of $T_1$ measurements [22]. The value obtained should be considered as an upper limit for the back charge transfer rate because we cannot exclude the possibility of having other kinds of free spins on the NMP stacks [23] — e.g. free radicals. The charge transfer on the TCNQ stacks in NMP TCNQ is thus estimated as $\rho = 1 - C \simeq 0.75$.

4. **Second moments and dipolar coupling determination.** — The electron-proton dipolar coupling gives rise to an angular dependent paramagnetic shift. In a powdered sample this does not contribute to the mean paramagnetic shift (first moment of the NMR line), but gives a second moment contribution which is proportional to the square of the susceptibility :

$$M_2 = \frac{4}{5}\left(\frac{\gamma_e}{\gamma_N}\right)^2 \chi^2 d^2 H^2 \qquad (2)$$

where $d^2$ is the effective square value of the dipolar electron-proton coupling. It is shown in the appendix that $d^2$ which enters in eq. (2) is exactly the same *effective square dipolar coupling* as that which is involved in the $T_1$ expression [24] for 1-D systems.

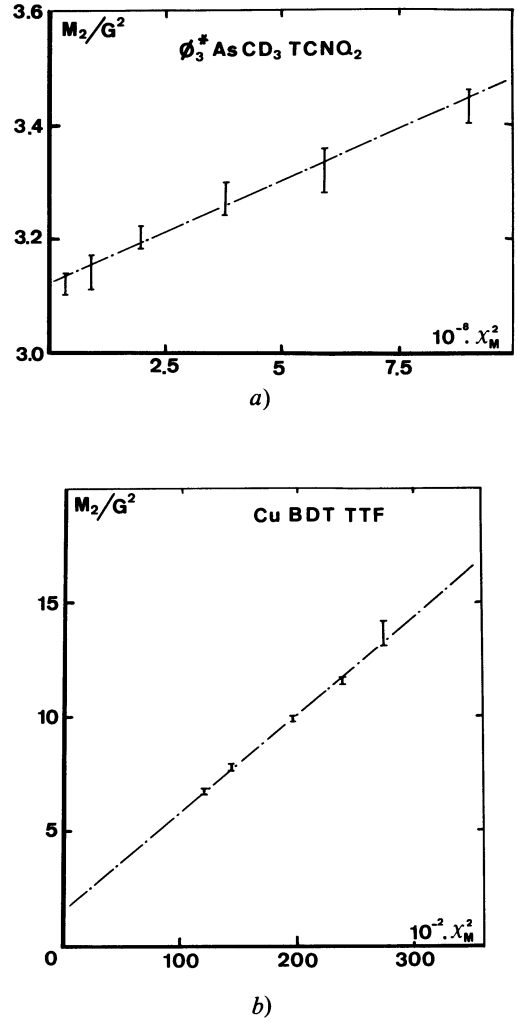


Fig. 3. — Proton NMR second moments of TCNQ (*a*) — TTF (*b*) — compounds as a function of the squared molar susceptibility.

The proton NMR line second moments are plotted *versus* $\chi^2$ in figures 3*b* and 3*a* for Cu BDT TTF and $\varphi_3^*$ $CD_3As\,TCNQ_2$, respectively. As explained in section 2, the variation of the second moment is known with a better accuracy than its absolute value. From this variation, one obtains :

$$d_F/\hbar \mid \gamma_e \mid = 0.67 \text{ G}$$

$$d_Q/\hbar \mid \gamma_e \mid = 0.60 \text{ G}$$

Table II. — *Scalar and dipolar electron-proton couplings for* TTF *and* TCNQ *in the solid state.*

| | TTF protons | | TCNQ protons | |
|---|---|---|---|---|
| | *a*/gauss | *d*/gauss | *a*/gauss | *d*/gauss |
| Experimental | − 1.2 | 0.67 | − 1.2 | 0.6 |
| Theoretical | | 0.66 (*) | | 0.65 (**) (1) 0.51 (**) (2) 0.58 (**) (3) |

(*) See text.

(**) See ref. [6]. Values (1), (2) and (3) have been obtained by assuming different sets of spin density distributions : (1) from ref. [25], (2) and (3) from ref. [9].

for the TTF and the TCNQ compound, respectively. The experimental $d_Q$ agrees very well with the results of extended calculations [6] performed for the same compound by considering its actual crystallographic structure and by assuming different models for the spin density distribution over the $TCNQ^-$ ion [9, 25] (see table II).

For Cu BDT TTF we have performed a calculation of $d_F$ by taking into account only the intra-molecular contribution. This approximation is certainly convenient for Cu BDT TTF where the inter-molecular distances between TTF ions are large (> 7.8 Å). In this calculation we have assumed a spin density distribution on the TTF molecule (Fig. 4) : $\sigma_s = 0.20$ spin on the sulphurs ; $\sigma_c = 0.05$ spin on the carbons adjacent to the protons. The latter comes from the experimental isotropic coupling assuming

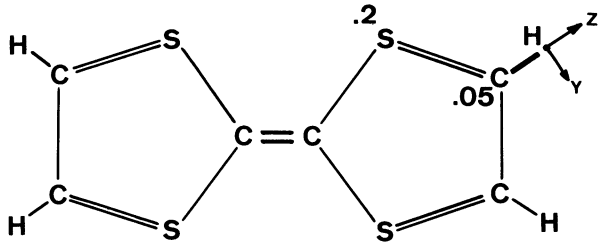


Fig. 4. — Spin density distribution in $TTF^+$.

[26] : $a = \sigma_c\ Q$ with $Q/\hbar\,|\,\gamma_e\,| = -23.4$ G. The former follows, neglecting the spin density on the two middle carbon atoms. The value $\sigma_s = 0.20$ is consistent with the result of a CNDO molecular orbital calculation (0.21). The protons have been assumed to be equivalent. The coupling of a given proton contains two parts :

i) A dipolar coupling arising from all the spin density points of the molecule except the adjacent carbon.

ii) A contact term of aromatic type due to the adjacent carbon. This coupling has been obtained by multiplying the aromatic coupling tensor, as determined in irradiated malonic acid [27], by the spin density $\sigma_c$. In its principal axis system $X$, $Y$, $Z$ (see Fig. 4) it is expressed as :

$$T = \begin{pmatrix} -1.2 & & \\ & -1.8 & \\ & & -0.6 \end{pmatrix}$$

where the principal values are given in gauss. Using eq. (A.19), one gets the theoretical value : $d_F = 0.66$ G, which is in excellent agreement with the experimental determination.

Let us point out that, contrary to the isotropic coupling $a$, the effective dipolar coupling $d$ is expected to be dependent on the structure, because it involves long range interactions. For instance, while it has been possible to consider only the intra-molecular contribution in Cu BDT TTF, it is expected that the inter-molecular contributions play a role in TTF TCNQ, where the TTF molecules are much nearer to each other (3.5 Å). Thus the TTF dipolar coupling in TTF TCNQ is expected to be (slightly) larger than 0.67 G. On the other hand, the value $d_Q = 0.60$ G as determined in $\varphi_3^*$ $AsCD_3$ $TCNQ_2$ probably works in other TCNQ salts, where the stacking is not too different.

One should notice that the couplings — scalar as well as dipolar — have been determined in salts where the charge transfer is complete. For compounds with incomplete charge transfer — like TTF TCNQ — the same values hold. In such cases, the incompleteness of the charge transfer is taken into account — e.g. in the expression of $T_1$ — by introducing the effective number of free spins : $kT\chi$ [4, 5, 28].

In conclusion, we emphasize that the dipolar electron-proton couplings in TTF and TCNQ are not negligible and should not be disregarded, in particular if one wants to perform a sound analysis of the $T_1$ data [28].

**Acknowledgments.** — We are greatly indebted to Mrs M. Guglielmi for the preparation of Qn* $TCNQ_2$ and NMP* TCNQ, and to L. V. Interrante and I. S. Jacobs who provided us with the Cu BDT TTF sample.

**Appendix I.** — EFFECTIVE DIPOLAR COUPLING. — We establish that the effective square dipolar couplings which are involved i) in the NMR line second moment, and ii) in the $T_1$ expression for low dimensional systems, are the same.

Let us consider a concentrated electronic spin system. In the site representation, the electronic spins $\mathbf{s}_\lambda$ are labelled by $\lambda$, the index of the cell. Let $\mathbf{i}_p$ be the nuclear spins (e.g. protons) of the cell located at the origin ($\lambda = 0$). There are $n_I$ inequivalent protons ($p = 1$ to $n_I$). The hyperfine interaction of the proton $p$ is written as :

$$H_p = \sum_\lambda \mathbf{i}_p\, \mathbf{T}_{p\lambda}\, \mathbf{s}_\lambda + \delta_{\lambda,0}\, a_p\, \mathbf{i}_p . \mathbf{s}_\lambda \qquad \text{(A.1)}$$

$a_p$ is the contact isotropic interaction of the proton $p$ with the spin of the origin cell. $\mathbf{T}_{p\lambda}$ is a traceless real symmetric tensor. It may be rewritten as :

$$\mathbf{T}_{p\lambda} = \mathbf{i}_p\, T_{p\lambda}\, \mathbf{s}_\lambda = \sum_{M=-2}^{+2} \mathbf{T}^M_{p\lambda} \qquad \text{(A.2)}$$

with :

$$\begin{aligned} \mathbf{T}^0_{p\lambda} &= t_{p\lambda}(\mathbf{h})\, \{\, 2 i^z_p\, s^z_\lambda - \tfrac{1}{2}(i^+_p\, s^-_\lambda + i^-_p\, s^+_\lambda)\,\} \\ \mathbf{T}^1_{p\lambda} &= -(\mathbf{T}^{-1}_{p\lambda})^* = -\sqrt{\tfrac{3}{2}}\, t^1_{p\lambda}(\mathbf{h})\, \{\, i^z_p\, s^-_\lambda + i^-_p\, s^z_\lambda \,\} \\ \mathbf{T}^2_{p\lambda} &= (\mathbf{T}^{-2}_{p\lambda})^* = \sqrt{\tfrac{3}{2}}\, t^2_{p\lambda}(\mathbf{h})\, i^-_p\, s^-_\lambda \end{aligned} \qquad \text{(A.3)}$$

where $t^M_{p\lambda}(\mathbf{h})$ are the components of spherical tensors

of order two, which depend on the field direction : $\mathbf{h} : \mathbf{H}/H$.

For a given direction of the field, the paramagnetic shift of the NMR line of the proton $p$ is :

$$\Delta H(\mathbf{h}) = \frac{\gamma_e}{\gamma_N} H\{ a_p + 2 \sum_\lambda t^0_{p\lambda}(\mathbf{h}) \} \qquad (A.4)$$

In a powdered sample, the first term gives a shift and the second a broadening of the line ; the corresponding first and second moments are :

$$\Delta H = \frac{\gamma_e}{\gamma_N} \chi H a_p$$
$$M_2 = 4\left(\frac{\gamma_e}{\gamma_N}\chi H\right)^2 \left\langle \left| \sum_\lambda t^0_{p\lambda}(\mathbf{h}) \right|^2 \right\rangle \qquad (A.5)$$

where the bracket means a spatial average over the direction of the field.

On the other hand, the nuclear relaxation rate of the proton $p$ is expressed as [24]

$$T_1^{-1} = \sum_\Lambda \{ A^\Lambda_z F^z_\Lambda(\omega_N) + A^\Lambda_+ F^+_\Lambda(\omega_e) \} \qquad (A.6)$$

where $\omega_N$ and $\omega_e$ are the nuclear and electronic Larmor angular frequencies, $F^\alpha_\Lambda(\omega)$ ($\alpha = z$ or $+$) is the frequency spectrum of the spin correlation function :

$$F^z_\Lambda(\omega) = \int_{-\infty}^{+\infty} dt\, e^{i\omega t} \langle s^z_\Lambda(t)\, s^z_{\lambda+\Lambda}(0) \rangle$$
$$F^+_\Lambda(\omega) = \tfrac{1}{2}\int_{-\infty}^{+\infty} dt\, e^{i\omega} \langle s^+_\Lambda(t)\, s^-_{\lambda+\Lambda}(0) \rangle \qquad (A.7)$$

and $A^\alpha_\Lambda$ are coupling constants which are related to the hyperfine interactions.

In 1-D systems, the main contribution to the relaxation at low frequencies comes from the long wavelength diffusive modes. In this hydrodynamic limit, the autocorrelation ($\Lambda = 0$) and crosscorrelation ($\Lambda \neq 0$) functions are the same : $F^\alpha_\Lambda(\omega) = F^\alpha(\omega)$, whatever $\Lambda$ connecting two sites in the same chain. If one defines : $A_\alpha = \sum_\Lambda A^\Lambda_\alpha$, the relaxation rate is then rewritten as :

$$T_1^{-1} = A_z F^z(\omega_N) + A_+ F^+(\omega_e) . \qquad (A.8)$$

Strickly speaking, this expression holds only for the long wavelengh contributions, which are dominant at low frequencies in low dimensional systems. However, as the main coupling comes from the site $\lambda = 0$, one expects : $A_\alpha \simeq A^0_\alpha$ ; thus eq. (A.8) should remain approximately valid in a more general case. For a powdered sample, one has to take the spatial averages of $A_\alpha$ which are expressed as :

$$\hbar^2 \langle A_z \rangle = 3 \left\langle \left| \sum_\lambda t^1_{p\lambda}(\mathbf{h}) \right|^2 \right\rangle$$
$$\hbar^2 \langle A_+ \rangle = a_p^2 + \left\langle \left| \sum_\lambda t^0_{p\lambda}(\mathbf{h}) \right|^2 \right\rangle + 6 \left\langle \left| \sum_\lambda t^2_{p\lambda}(\mathbf{h}) \right|^2 \right\rangle . \qquad (A.9)$$

Let us now calculate

$$X_M = \left\langle \left| \sum_\lambda t^M_{p\lambda}(\mathbf{h}) \right|^2 \right\rangle .$$

Let $\mathbf{z}$ be a given direction of the crystal. $\mathbf{h}$ may transform into $\mathbf{z}$ by a rotation $R$ : $\mathbf{z} = R\mathbf{h}$. In the rotation, the components of the spherical tensor are transformed, according to the irreducible representation $D_2$ of the rotation group :

$$t^M_{p\lambda}(\mathbf{h}) = \sum_{M'} D_2^{MM'}(R)\, t^{M'}_{p\lambda}(\mathbf{z}) \qquad (A.10)$$

where $D_2^{MM'}(R)$ is the matrix element of $D_2(R)$. Then it follows :

$$X_M = \sum_{\lambda\mu} \sum_{M'M''} \langle D_2^{MM'}(R)\, D_2^{MM''}(R)^* \rangle\, t^{M'}_{p\lambda}(\mathbf{z})\, t^{M''}_{p\mu}(\mathbf{z})^* . \qquad (A.11)$$

The spatial average is equivalent to a summation over all the elements of the rotation group. It yields :

$$X_M = \frac{1}{5}\sum_{M'} \left| \sum_\lambda t^{M'}_{p\lambda}(\mathbf{z}) \right|^2 . \qquad (A.12)$$

Thus it turns out that $X_M$ is independent of $M$. If one defines :

$$d_p^2 = \sum_M \left| \sum_\lambda t^M_{p\lambda}(\mathbf{z}) \right|^2 \qquad (A.13)$$

it appears that the same effective dipolar coupling $d_p^2$ occurs in the expressions of the second moment (A.6) as well as for the nuclear relaxation rate (A.9) in powders.

Now, if one takes into account the $n_I$ inequivalent protons, one obtains :

$$\Delta H = \frac{\gamma_e}{\gamma_N} \chi H \bar{a}$$
$$M_2 = \left(\frac{\gamma_e}{\gamma_N}\chi H\right)^2 (a^2 - \bar{a}^2 + 4/5\, d^2) \qquad (A.14)$$
$$\hbar^2 \langle A_z \rangle = 3/5\, d^2$$
$$\hbar^2 \langle A_+ \rangle = a^2 + 7/5\, d^2$$

where we have defined :

$$\bar{a} = n_I^{-1} \sum_p a_p$$
$$a^2 = n_I^{-1} \sum_p a_p^2 \qquad (A.15)$$
$$d^2 = n_I^{-1} \sum_p d_p^2 .$$

Finally, we give the actual expression to calculate $d_p$. To describe the hyperfine coupling, one considers a spin density distribution : each electronic spin $\mathbf{s}_\lambda$ is delocalized over several points $\lambda_i$ ($i = 1$ to $n_s$) with spin density $\sigma_i$ $\left(\sum_i \sigma_i = 1\right)$. The hyperfine interaction

results from the superposition of the dipolar interaction between the proton $p$ and the spin density $\sigma_i$ at the point $\lambda_i$ :

$$t^M_{p\lambda}(\mathbf{z}) = \sqrt{\frac{4\pi}{5}} \sum_i d_{p\lambda_i} Y^M_2(\mathbf{r}_{p\lambda_i}) \qquad (A.16)$$

where $\mathbf{r}_{p\lambda_i}$ is the vector joining the proton $p$ to the point $\lambda_i$, $Y^M_2(\mathbf{x})$ is the spherical harmonic related to the direction $\mathbf{x}$ and $d_{p\lambda_i}$ is the partial dipolar coupling :

$$d_{p\lambda_i} = \sigma_i \frac{\hbar^2 \mid \gamma_e \mid \gamma_N}{r^3_{p\lambda_i}}. \qquad (A.17)$$

However, when the proton is very near the spin density point ($r_{p\lambda_i} < 2$ Å), a more general tensor should be used instead of the dipolar one. Actually this contact tensor can be decomposed in a general way into an isotropic term and three dipolar tensors. Thus eq. (A.16) remains valid, provided one takes into account these three dipolar couplings in place of the anisotropic part of the contact tensor.

From eq. (A.13) and (A.16), $d_p$ is then expressed as :

$$d_p^2 = \frac{4\pi}{5} \sum_M \sum_{\substack{\lambda\mu \\ ij}} d_{p\lambda_i} d_{p\mu_j} Y^M_2(\mathbf{r}_{p\lambda_i}) Y^M_2(\mathbf{r}_{p\mu_j})^* \qquad (A.18)$$

Using the addition theorem for the spherical harmonics, one obtains :

$$d_p^2 = \sum_{\substack{\lambda\mu \\ ij}} d_{p\lambda_i} d_{p\mu_j} P_2(\cos(\mathbf{r}_{p\lambda_i}, \mathbf{r}_{p\mu_j})) \qquad (A.19)$$

where $P_2(x) = (3x^2 - 1)/2$.

## References


[1] BUTLER, M. A., WUDL, F. and SOOS, Z. G., *Phys. Rev.* **B 12** (1975) 4708.

[2] RYBACZEWSKI, E. F., SMITH, L. S., GARITO, A. F. and HEEGER, A. J., *Phys. Rev.* **B 14** (1976) 2746.

[3] DEVREUX, F., *Phys. Rev.* **B 13** (1976) 4651.

[4] SODA, G., JEROME, D., WEGER, M., ALIZON, J., GALLICE, J., ROBERT, R., FABRE, J. M. and GIRAL, L., *J. Physique* **38** (1977) 931.

[5] EHRENFREUND, E. and HEEGER, A. J., *Solid State Commun.* **24** (1977) 29.

[6] AVALOS, J., Thèse de 3e cycle, Grenoble (1977).
AVALOS, J., DEVREUX, F., GUGLIELMI, M. and NECHTSCHEIN, M., *Mol. Phys.* **36** (1978) 669.

[7] ABRAGAM, A., *Les principes du Magnétisme Nucléaire* (PUF) 1961, p. 209.

[8] *Idem*, réf. [7], p. 223.

[9] LOWITZ, D. A., *J. Chem. Phys.* **46** (1967) 4698.

[10] JACOBS, I. S., BRAY, J. W., HART, H. R., INTERRANTE, L. V., KASPER, J. S., WATKINS, G. D., PROBER, D. E. and BONNER, J. C., *Phys. Rev.* **B 14** (1976) 3036.

[11] KEPLER, R. G., *J. Chem. Phys.* **39** (1963) 3528.

[12] WUDL, F., SMITH, G. M. and HUFNAGEL, E. J., *Chem. Commun.* **21** (1970) 1453.

[13] FISCHER, P. H. and MACDOWELL, C. A., *J. Am. Chem. Soc.* **85** (1963) 2694.

[14] KUINDERSMA, P. I., thesis, Groningen (1975) unpublished.

[15] SHCHEGOLEV, I. F., MAKOVA, M. K., FEDUTIN, D. N., KRAINSKII, I. S., KHIDEKEL, M. L. and YAGUBSKII, E. B., *Sov. Phys. JETP* **45** (1977) 596.

[16] SHCHEGOLEV, I. F. and BULAEVSKII, L. N., *Proc. of the Conf. on quasi* — 1-D — *conductors*, Dubrovnick (1978), to be published.

[17] EHRENFREUND, E. and GARITO, A. F., *Solid State Commun.* **19** (1976) 815.

[18] DEVREUX, F., unpublished work.

[19] SANNY, J. and CLARK, W. G., *Proc. of the Conf. on quasi* — 1-D — *conductors*, Dubrovnick (1978), to be published.

[20] TOMKIEWICZ, Y., JATANKO, A. R. and TORRANCE, J. B., *Phys. Rev. Lett.* **36** (1976) 751.

[21] RYBACZEWSKI, E. F., SMITH, L. S., GARITO, A. F. and HEEGER, A. T., *Phys. Rev.* **B 14** (1976) 2746.

[22] DEVREUX, F., GUGLIELMI, M. and NECHTSCHEIN, M., *J. Physique* **39** (1978) 541.

[23] SOOS, Z. G., KELLER, H. J., MORONI, W. and NÖTHE, D., *J. Am. Chem. Soc.* **99 : 15** (1977) 5040.

[24] DEVREUX, F., BOUCHER, J. P. and NECHTSCHEIN, M., *J. Physique* **35** (1974) 271.

[25] JONKMAN, H. T., VAN DER VELDE, G. A. and NIEUWPOORT, W. C., *Chem. Phys. Lett.* **25** (1974) 62.

[26] MCCONNELL, H. M., *J. Chem. Phys.* **24** (1956) 632.
HIGUGHI, J., *J. Chem. Phys.* **39** (1962) 3455.

[27] MCCONNELL, H. M., HELLER, C., COLE, T. and FESSENDEN, R. W., *J. Am. Chem. Soc.* **82** (1960) 766.

[28] DEVREUX, F. and NECHTSCHEIN, M., *Proc. of the Conf. on quasi* — 1-D — *conductors*, Dubrovnick (1978), to be published.